THE INFLUENCE OF STRATOSPHERIC WINDS ON A SUSPENDED INSTRUMENT PACKAGE

By M. N. Brearley*

[*Manuscript received August* 16, 1968]

Summary

One of many high altitude experiments performed by the Physics Department of the RAAF Academy (Hopper *et al.* 1963) involves a small instrument package suspended from a balloon on a fine nylon yarn several miles long. Any wind shear that exists between the balloon and package will induce a relative lateral displacement by way of air drag on the yarn and package. This paper establishes the package displacements and yarn shapes produced by several wind shears of simple profiles, and suggests a method by which our knowledge of wind structure in the stratosphere may be extended. Numerical results are included for a typical situation involving a balloon at an altitude of 90 000 ft and a yarn about 4 miles in length.

The analysis makes use of information, previously unavailable, on the air drag characteristics of woven nylon yarns at moderately low Reynolds numbers ($2 \leqslant R \leqslant 100$); the data required were obtained experimentally using apparatus specially designed and built for the purpose.

I. Introduction

The procedure followed in experiments in which an instrument package is suspended from a stratospheric balloon by several miles of nylon yarn is as follows: As the balloon approaches its prescribed altitude a pressure-actuated (or pre-set clockwork) device releases the package, which falls under gravity and unwinds from a cone the fine yarn to which it is attached. The process of descent of the package and yarn is aerodynamically interesting and will be discussed in a subsequent paper.

This paper investigates as separate problems: (1) the static vertical extension of the elastic yarn under its own weight and that of the package, and (2) the relative horizontal displacement of balloon and package resulting from a wind shear existing between them. The latter problem requires knowledge of the air drag force on the yarn at high altitudes as a function of the velocity of the air flow, and since the woven filament construction of the yarn gives it a rough exterior precluding its treatment as a smooth cylinder, experimental methods are needed to determine its drag coefficient. Apparatus was designed and built for this purpose, and an extensive testing programme was undertaken to establish values of the drag coefficient for both normal and inclined air flows over a range of Reynolds number appropriate to the high altitude situation.

* RAAF Academy, RAAF Base, Point Cook, Vic. 3029.

II. Effects of Static Extension of Yarn

The notation depicted in Figure 1 will be used, with w_0 being the weight per unit length of the unstretched yarn and λ the elastic modulus of the yarn (corrected for low temperature effect in the stratosphere). An extensiometer test on the yarn established the value of λ and showed it to be constant up to the yarn failure load. Hook's law therefore applies, so that the equation of equilibrium of the element dx of yarn depicted in Figure 1 may be written (Ramsey 1945)

$$W+w_0x_0 = T = \lambda(dx-dx_0)/dx_0. \tag{1}$$

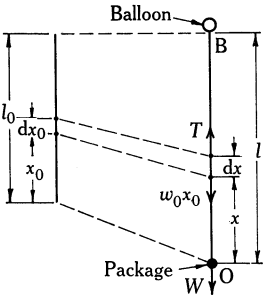

Fig. 1.—Effect of weights of yarn and instrument package in stretching the yarn from natural length l_0 to length l.

The solution of this differential equation satisfying the condition that x and x_0 vanish together is

$$x = x_0+(W/\lambda)x_0+\tfrac{1}{2}(w_0/\lambda)x_0^2.$$

Putting $x_0 = l_0$ gives the extended length of the yarn as

$$l = l_0+(W/\lambda)l_0+\tfrac{1}{2}(w_0/\lambda)l_0^2. \tag{2}$$

The variations in the diameter d and the weight per unit length w of the yarn are worth investigating, in case their departures from their unstretched values d_0 and w_0 are large enough to affect the lateral deflection problem. Conservation of the mass of the yarn element in Figure 1 shows that

$$w\,dx = w_0\,dx_0,$$

and on using (1) this gives

$$w = w_0\{1+(W+w_0x_0)/\lambda\}^{-1}.$$

At the highest point $x_0 = l_0$, w takes its least value

$$w_{\min} = w_0\{1+(W+w_0l_0)/\lambda\}^{-1}. \tag{3}$$

Since w evidently varies as d^2 along the yarn,

$$w/w_0 = d^2/d_0^2,$$

and from (3) it follows that the least yarn diameter is

$$d_{\min} = d_0\{1+(W+w_0l_0)/\lambda\}^{-\frac{1}{2}}. \tag{4}$$

Numerical Values in a Typical Particular Case

In a typical experiment a balloon at an altitude of 90 000 ft supports a package on a yarn of natural length

$$l_0 = 20\,000 \text{ ft} = 6096 \text{ m}.$$

A yarn that is in common use is a singly woven multifilament 840 denier type (1 denier = mass in grams of 9000 m of yarn). Because of the twist given to the yarn during manufacture, the denier specification is not accurate enough as a measure of w_0, and by weighing a sample of the unstretched yarn it was found that

$$w_0 = 1{\cdot}010 \times 10^{-4} \text{ kg wt m}^{-1} = 9{\cdot}90 \times 10^{-4} \text{ N m}^{-1}.$$

The total weight of the yarn is

$$w_0 l_0 = 1{\cdot}36 \text{ lb wt} = 0{\cdot}616 \text{ kg wt} = 6{\cdot}03 \text{ N}.$$

It was found experimentally that $\lambda = 16{\cdot}8$ kg wt at 20°C. The yarn manufacturers suggest (Fibremakers Ltd 1951) a factor of 1·61 to modify λ to allow for the atmospheric temperature of about −56°C in the region spanned by the yarn, so that

$$\lambda = 27{\cdot}0 \text{ kg wt} = 265 \text{ N}.$$

Measurements with a travelling microscope gave the yarn diameter

$$d_0 = 0{\cdot}446 \text{ mm} = 4{\cdot}46 \times 10^{-4} \text{ m}.$$

A typical instrument package consists of a rectangular box with top 6 in. by 6 in., depth 8 in., and weight

$$W = 2{\cdot}0 \text{ lb wt} = 0{\cdot}907 \text{ kg wt} = 8{\cdot}89 \text{ N}.$$

The numerical form of equation (2) for this case is

$$l = 6096 + 205 + 70 \text{ m} = 6371 \text{ m} = 20\,900 \text{ ft}.$$

The package and yarn weights increase the natural yarn length l_0 by 3·4% and 1·1% respectively, and stretch it by 900 ft.

The numerical forms of (3) and (4) are respectively

$$w_{\min} = 0{\cdot}947\, w_0, \qquad d_{\min} = 0{\cdot}973\, d_0.$$

The reductions in w_0 and d_0 due to yarn extension are small enough to be neglected in the succeeding analysis.

III. Equilibrium Equations of System under Wind Shear

In describing the deflected shape of the yarn under transverse wind loads (Fig. 2), the lowest point of the yarn is taken as origin O and a general point P of the yarn is taken to have Cartesian coordinates (x, y) and intrinsic coordinates (s, ψ), where s is the arc length OP of the yarn.

In Figure 2, $v(x)$ denotes the velocity (assumed horizontal) of the air relative to the balloon at a general height x above O. The functional form of the velocity profile $v(x)$ will not be particularized until Section IX. Evidently $v(x)$ vanishes at the balloon, say at $x = l_1$, where l_1 is the vertical height of the balloon above the instrument package.

The forces shown in Figure 2 include D_W, the air drag on the instrument package, $w\,\mathrm{d}s$, the weight of an element of yarn of length ds, $F\,\mathrm{d}s$, the air drag on the element ds of yarn, and T, the tension in the yarn at the point P. It is shown in Section IV that F is parallel to $v(x)$, and so horizontal in the case shown in Figure 2.

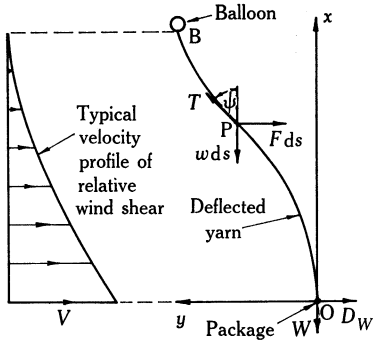

Fig. 2.—Typical velocity profile of wind shear relative to the balloon; and deflected yarn with forces T, W, and D_W on the portion OP and forces $F\,\mathrm{d}s$ and $w\,\mathrm{d}s$ on the element ds at P.

The horizontal and vertical components of the equations of relative equilibrium of the portion OP of the system in Figure 2 are

$$T\sin\psi = D_W + \int_0^s F\,\mathrm{d}s\,, \tag{5}$$

and

$$T\cos\psi = W + \int_0^s w\,\mathrm{d}s\,. \tag{6}$$

On dividing (5) by (6) and using $\tan\psi = \mathrm{d}y/\mathrm{d}x$ and the fact that w may be taken as constant, one obtains

$$\mathrm{d}y/\mathrm{d}x = (W+ws)^{-1}\left(D_W + \int_0^s F\,\mathrm{d}s\right). \tag{7}$$

In Section V the right member of (7) is obtained as a function of x. The shape $y(x)$ of the deflected yarn may then be found by integrating (7) subject to the initial condition

$$y(0) = 0\,. \tag{8}$$

IV. Determination of Air Drag Force F on Yarn

(a) *Use of Hydrodynamics Similarity Theory*

For a circular cylinder of diameter d with its axis held perpendicular to a uniform stream of fluid of density ρ and velocity v, the drag coefficient per unit length is defined (Goldstein 1952) to be

$$C_D = D/\tfrac{1}{2}\rho v^2 d\,, \tag{9}$$

where D is the drag force per unit length on the cylinder. The Reynolds number R of the flow situation is defined as

$$R = vd/\nu, \tag{10}$$

where ν is the kinematic viscosity of the fluid.

For different flow situations that are geometrically similar it is well known that C_D is the same function of R, say

$$C_D = f(R). \tag{11}$$

In general the functional form f varies with R and (in the present context) with cylinder shape, and must usually be determined by experiment. The value of knowing f lies in the fact that (9), (10), and (11) then enable D to be found explicitly from

$$D = \tfrac{1}{2}\rho v^2 d f(vd/\nu) \tag{12}$$

for all values of v, d, and ν corresponding to Reynolds numbers lying in the interval of R for which the function f has been found.

To ensure that the laboratory experiments to find f do cover the interval of R relevant to the stratospheric situation, the anticipated bounds of R are found from (10). For illustrative purposes it will be assumed that the wind shear velocity relative to the yarn ranges from zero to 50 knots. For a yarn lying between 70 000 and 90 000 ft altitude, the least value of ν for air occurs at the lower altitude and is found from tables of atmospheric properties (Gray 1963) to be $2{\cdot}0\times10^{-4}$ m^2 sec^{-1}. For the yarn described in Section II the relevant range of Reynolds number is found from (10) to be

$$0 \leqslant R \leqslant 57, \tag{13}$$

and this range must be covered in the laboratory experiments used to determine the form of the function f in (11) and (12).

(*b*) *Determination of Normal Air Drag on Yarn*

Two different sets of experiments were performed to enable the air drag per unit length of the yarn to be determined as a function of air flow velocity for relative air flows that were (1) perpendicular to the yarn, and (2) inclined to the yarn at various angles. The arrangements used in these two sets of experiments are shown schematically in Figures 3(*a*) and 3(*b*) respectively.

In both Figures 3(*a*) and 3(*b*), AB represents a moving continuous belt of nylon yarn which runs around pulleys at A and B and is driven by an electric motor at a speed v that can be varied; O denotes a point of this moving belt at which is attached a sample OC of length L of the yarn whose drag is to be measured. The velocity v can be found by measuring the time taken for OC to perform one circuit of known length 2AB. It is to be expected that the yarn OC (which is uniform) will settle down to a straight shape during its progress along BA if v remains constant, and this behaviour was observed during the experiments.

In Figure 3(*a*) the angle of inclination α of AB is adjusted so that the moving yarn OC remains perpendicular to AB under the influence of its weight wL and the

air drag force DL, where D is the normal drag force per unit length of yarn since the relative air velocity v is perpendicular to OC. From the equation of motion of the yarn, or by taking moments about O in Figure 3(a), it is seen that

$$D = w \sin \alpha . \tag{14}$$

Since w is known and α can be measured, (14) enables D to be determined over any selected range of values of v.

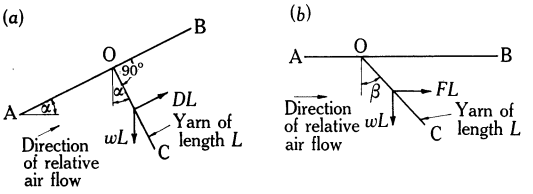

Fig. 3.—Drag experiments producing relative air flows (a) perpendicular to the yarn, (b) inclined to the yarn.

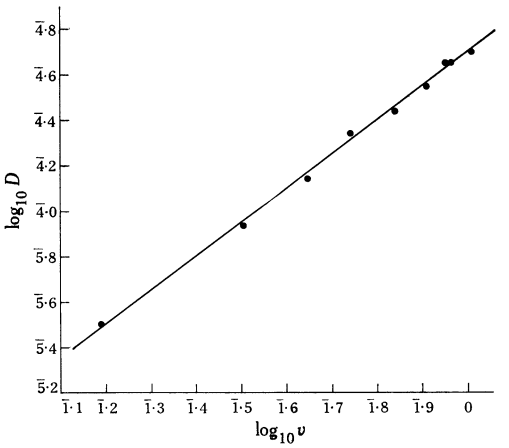

Fig. 4.—Relation between $\log_{10} D$ and $\log_{10} v$ for normal air flow past 840 denier woven nylon yarn, where D (N m^{-1}) is the normal drag force and v (m sec^{-1}) is the flow velocity.

The normal drag was determined in this way for the yarn described in Section II, and the values found for $\log D$ were plotted against those of $\log v$ (Fig. 4). As their distribution appears linear, a straight line of the form

$$\log D = \log D_0 + m \log v \tag{15}$$

was fitted to them visually, and it was found that

$$m = 1 \cdot 501, \qquad \log D_0 = \bar{4} \cdot 70 . \tag{16}$$

From the form of equation (15) it is easily seen that (11) must be a linear relation between $\log C_D$ and $\log R$, say

$$\log C_D = \log k - n \log R , \tag{17}$$

where k and n are constants. By (9) and (10) this may be written

$$\log D = \log(\tfrac{1}{2}\rho d) + \log k - n \log(d/\nu) + (2-n) \log v . \tag{18}$$

On comparing (15) and (18) it is seen that

$$n = 2-m \tag{19}$$

and thus

$$\log k = \log D_0 - \log(\tfrac{1}{2}\rho d) + n \log(d/\nu). \tag{20}$$

Numerical values of n and k for the yarn of Section II may now be obtained. The laboratory experiments were performed at sea level at 20°C, for which the density and kinematic viscosity of air are (Gray 1963)

$$\rho = 1{\cdot}205 \text{ kg m}^{-3}, \qquad \nu = 1{\cdot}50 \times 10^{-5} \text{ m}^2 \text{ sec}^{-1}, \tag{21}$$

while the yarn diameter d is $4{\cdot}46 \times 10^{-4}$ m. From (16), (19), (20), and (21) it is found that

$$n = 0{\cdot}499 \simeq 0{\cdot}5, \qquad k = 10{\cdot}14. \tag{22}$$

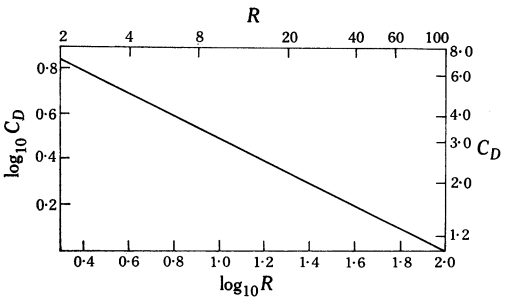

Fig. 5.—Variation of drag coefficient C_D with Reynolds number R for 840 denier woven nylon yarn in the range $2 \leqslant R \leqslant 100$.

The numerical equivalent of the exponential form of (17) is

$$C_D = kR^{-n} = 10{\cdot}14\, R^{-0{\cdot}5}. \tag{23}$$

Equation (23) is the form taken by (11) in the present context. The corresponding form of (12) is seen to be

$$D = \tfrac{1}{2}k\rho\nu^n d^{1-n} v^{2-n} = 0{\cdot}107\, \rho\nu^{1/2} v^{3/2}. \tag{24}$$

The numerical form of (17) is

$$\log C_D = 1{\cdot}006 - 0{\cdot}5 \log R, \tag{25}$$

which is represented graphically in Figure 5 over the range

$$2 \leqslant R \leqslant 100 \tag{26}$$

of Reynolds numbers. This extension of the range $4{\cdot}6 \leqslant R \leqslant 31$ that was covered by tests on the 840 denier yarn was achieved by other tests on similar woven yarns of both smaller and larger diameters. The increased range (26) is the range of validity of (23) and (24); it does not extend down to zero as required in (13), but the error involved in assuming it to do so will be negligible for practical purposes since the air drag forces on the yarn will be trivial at the small flow velocities involved.

(c) *Determination of Air Drag on Inclined Yarn*

The second set of experiments depicted in Figure 3(*b*) is now considered. As the point O moves along BA, the yarn OC is blown back at an angle β to the vertical which depends on the yarn weight wL and the air drag force FL, where F is the drag force per unit length on the inclined yarn.

Although the force FL has been shown as horizontal in Figure 3(*b*), it is not obvious that this is correct. In general, F will not be exactly horizontal, and the extent of its deviation from this direction depends upon the Reynolds number R of the flow. For values of R appropriate to the experiment considered in this paper, the deviation of F from the horizontal is small enough to be ignored. This is a consequence of an independence principle (Sears 1948) deducible from the Navier–Stokes equations of the flow past a yawed cylinder. Because the mathematical derivation of this principle gives no indication of the range of Reynolds number for which it is valid, and because of its importance in the solution of the problem under discussion, the validity of the principle in the present context was tested experimentally in the following way.

On the assumption that FL in Figure 3(*b*) is a horizontal force, taking moments about O is seen to give

$$F = w \tan \beta . \tag{27}$$

Measurements of β therefore enable F to be determined over any desired range of values of v. One of the results that follows from the independence principle is that the forces D and F in Figures 3(*a*) and 3(*b*) are related (for the same relative air velocity v) by the equations

$$F = D \cos \beta , \qquad D = F \sec \beta . \tag{28a, 28b}$$

To test the accuracy of (28a, 28b) (and hence the validity of the independence principle), the experimental values of $\log(F \sec \beta)$ are plotted against $\log v$, using the values of F obtained from (27) for various angles β; and on the same graph we plot the normal flow data $\log D$ versus $\log v$ which were used to produce Figure 4. According to (28b), these two sets of points should lie on the same locus; and conversely, if they do so, equations (28a, 28b) and the principle on which they were based survive a test of validity in the range of R over which the experiments were made.

The result of superposing the two sets of points is shown in Figure 6, and the correspondence between them is seen to be close. This process has been carried out for numerous yarns for Reynolds numbers slightly beyond 100, with good correspondence in every case. The details of this and allied work will be reported in more detail in a later paper. The foregoing test of the independence principle is not a complete one, but it indicates that equations (28a, 28b) may be used with confidence under the conditions of the problem considered here.

Figure 2 shows that in the balloon experiment the angle ψ must be used for β in equations (28a, 28b). Then substitution for D from (24) in (28a) gives

$$F = \tfrac{1}{2} k \rho \nu^n d^{1-n} v^{2-n} \cos \psi = 0 \cdot 107 \, \rho \nu^{1/2} v^{3/2} \cos \psi . \tag{29}$$

Equation (29) gives the air drag per unit length of the yarn at the general point P in Figure 2, provided that ρ and ν are given their correct values at P, and v is taken as the relative wind shear velocity $v(x)$ at that point.

V. Differential Equation of Yarn Deflection Curve

The slope of the yarn at the point P in Figure 2 is given by equation (7). In the integral term the form of F in (29) may be used, and the variable of integration transformed to x by the relation $\mathrm{d}x = \mathrm{d}s\cos\psi$, giving

$$\mathrm{d}y/\mathrm{d}x = (W+ws)^{-1}\left(D_W+\tfrac{1}{2}kd^{1-n}\int_0^x \rho v^n v^{2-n}\,\mathrm{d}x\right). \tag{30}$$

Resisting the temptation to make the obvious approximation $s \simeq x$ in (30) (and so restricting its validity to nearly vertical yarns), we introduce instead the dimensionless variable

$$X = x/l_1, \tag{31}$$

where l_1 is the vertical depth of the package below the balloon (Fig. 2).

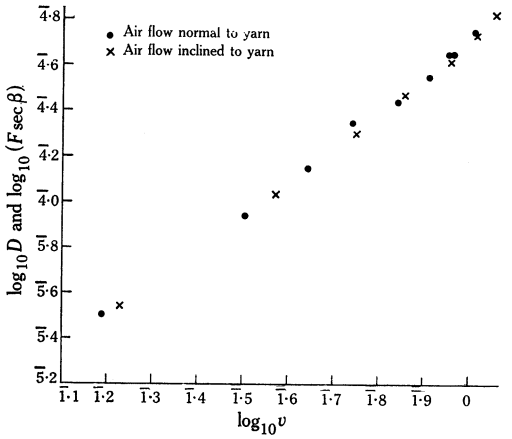

Fig. 6.—Test of the validity of Sears independence principle for $2 \leqslant R \leqslant 100$ by superposition of points of $\log_{10} D$ versus $\log_{10} v$ for normal air flow and $\log_{10}(F\sec\beta)$ versus $\log_{10} v$ for flow inclined at an angle β to the woven nylon yarn.

Figure 2 shows that provided the curvature of the deflected yarn is not excessive it is a reasonable approximation to take

$$s = (l/l_1)x = lX. \tag{32}$$

In using (32) the limitation that $\mathrm{d}^2y/\mathrm{d}x^2$ be small is accepted, but a similar restriction on $\mathrm{d}y/\mathrm{d}x$ is avoided.

Substitution from (31) and (32) in (30) gives

$$\mathrm{d}y/\mathrm{d}X = l_1(W+wlX)^{-1}(D_W+D_X), \tag{33}$$

where

$$D_X = \tfrac{1}{2}kd^{1-n}l_1\int_0^X \rho v^n v^{2-n}\,\mathrm{d}X, \tag{34}$$

and is the lateral air drag force on the yarn in the range $(0, X)$. In equation (33), y denotes $y(X)$, and in (34) the integrand is supposed expressed as a function of X.

On writing $W_1 = wl$ as the total weight of the whole yarn and $\alpha = W/W_1$ as the ratio of weights of package and whole yarn, equation (33) takes the form

$$\mathrm{d}y/\mathrm{d}X = (l_1/W_1)(X+\alpha)^{-1}(D_W+D_X). \tag{35}$$

The initial condition $y(0) = 0$ of equation (8) is still relevant in terms of the new variable X.

Before seeking the solution of (35) the forms of the drag forces D_W and D_X are considered.

VI. Air Drag D_W on Suspended Package

The drag coefficient for an obstacle such as the package in an air stream of velocity V and density ρ is defined (Goldstein 1952) as

$$C_D = D_W/\tfrac{1}{2}\rho V^2 S, \tag{36}$$

where S is the cross sectional area of the obstacle in the flow.

The Reynolds number of the flow is defined to be

$$R = VS^{1/2}/\nu, \tag{37}$$

where ν is the kinematic viscosity of the air at the obstacle.

Equation (36) enables C_D to be determined experimentally for the instrument package by a method described in Appendix I. For the package described in Section II it was found that

$$S = 48 \text{ in}^2 = 0{\cdot}0310 \text{ m}^2, \qquad C_D = 1{\cdot}26, \tag{38}$$

this value of C_D being constant for the situations considered here, as explained in Appendix I. Equation (36) yields the air drag force on the package as

$$D_W = \tfrac{1}{2}C_D \rho_0 S V^2, \tag{39}$$

where ρ_0 is the air density at the altitude of the package.

VII. Air Drag on Deflected Nylon Yarn

In equation (34) for the yarn drag we may use the definition

$$\nu = \mu/\rho, \tag{40}$$

where μ is the viscosity coefficient of the air. Since μ is virtually independent of altitude in that part of the stratosphere in which we are interested, this gives the drag on the yarn in the height interval corresponding to $(0, X)$ as

$$D_X = \tfrac{1}{2}kd^{1-n}\mu^n l_1 \int_0^X \rho^{1-n} v^{2-n}\, \mathrm{d}X. \tag{41}$$

In (41), the air density ρ may be found from tables of atmospheric properties, and v may be any particular wind shear velocity profile whose effects we wish to investigate.

At this stage the general value of n occurring in the exponents in (41) will be abandoned in favour of the value $0{\cdot}5$ (equation (22)) which it takes for the particular experiment considered here, the modifications needed in the sequel for other values of n being obvious. The relevant form of (41) is now

$$D_X = \beta l_1 \int_0^X \rho^{1/2} v^{3/2}\, \mathrm{d}X, \tag{42}$$

where

$$\beta = \tfrac{1}{2}kd^{1/2}\mu^{1/2} = \text{constant}. \tag{43}$$

Without sacrificing useful information on the relation between wind shear structure and deflected yarn shape the evaluation of the integral in (42) may be made analytically simple by taking the integrand to have the form

$$\rho^{1/2}v^{3/2} = \rho_0^{1/2}V^{3/2}(1-X)^p, \tag{44}$$

where p is a constant and ρ_0 and V are values of ρ and v at the instrument package ($X = 0$). The corresponding relative wind shear velocity profile is

$$v = V(\rho_0/\rho)^{1/3}(1-X)^{2p/3}, \qquad 0 \leqslant X \leqslant 1. \tag{45}$$

By varying the parameter p a family of profiles may be generated.

From (42) and (44) it is easily seen that (if $p \neq -1$)

$$D_X = \beta l_1 \rho_0^{1/2} V^{3/2}(p+1)^{-1}\{1-(1-X)^{p+1}\}. \tag{46}$$

In particular, the air drag on the whole yarn (up to $X = 1$) is

$$D_1 = \beta l_1 \rho_0^{1/2} V^{3/2}(p+1)^{-1}. \tag{47}$$

In Section IX the profiles for which p is a positive integer are considered, for which (46) may be written

$$D_X = \beta l_1 \rho_0^{1/2} V^{3/2} \sum_{r=1}^{p+1} (-)^{r+1} A_{pr} X^r, \tag{48}$$

where

$$A_{pr} = \binom{p+1}{r}(p+1)^{-1}. \tag{49}$$

The profiles are plotted for $p = 1$, 2, and 3 and the corresponding deflected yarn shapes are determined.

In Section X the profiles (45) (which have continuous slopes) are replaced by step-function forms to represent wind shears having sharp slope discontinuities.

VIII. Deflection Curve of Yarn under Wind Shears

Equation (35) will now be integrated to yield the equation of the yarn deflection curve for the wind shear profiles of equation (45). On using the forms of D_W and D_X from equations (39) and (48), equation (35) may be written

$$\mathrm{d}y/\mathrm{d}X = l_1(X+\alpha)^{-1}\left(aV^2 + cl_1 V^{3/2} \sum_{r=1}^{p+1} (-)^{r+1} A_{pr} X^r\right), \tag{50}$$

where the constants a and c are defined by

$$a = \tfrac{1}{2}C_D \rho_0 S/W_1, \qquad c = \beta\rho_0^{1/2}/W_1. \tag{51}$$

On introducing the new independent variable

$$\xi = X+\alpha \tag{52}$$

in (50), and making an obvious binomial expansion in the last term, this differential

equation becomes

$$\mathrm{d}y/\mathrm{d}\xi = l_1^2\left(cV^{3/2}\sum_{r=1}^{p+1}\sum_{s=1}^{r} B_{prs}\,\xi^{s-1} - (cb_p\,V^{3/2} - al_1^{-1}\,V^2)\xi^{-1}\right), \tag{53}$$

where y now denotes $y(\xi)$ and

$$B_{prs} = (-)^{r+1}A_{pr}\binom{r}{s}(-\alpha)^{r-s}, \tag{54}$$

$$b_p = \sum_{r=1}^{p+1} A_{pr}\,\alpha^r. \tag{55}$$

Equation (53) may now be integrated with respect to ξ and the resulting integration constant evaluated from the initial condition (8), which in terms of $y(\xi)$ takes the form

$$y(\alpha) = 0. \tag{56}$$

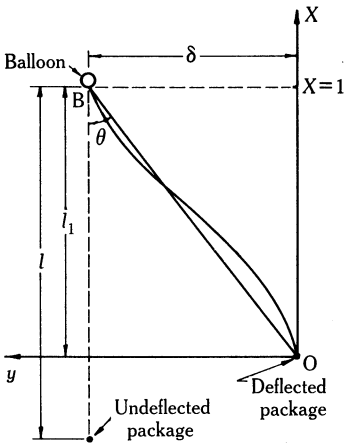

Fig. 7.—Angular deflection θ, horizontal deflection δ, and vertical displacement l_1 of the package relative to the balloon.

With the aid of the binomial expansion

$$(X+\alpha)^s - \alpha^s = \alpha^s \sum_{t=1}^{s}\binom{s}{t}\alpha^{-t}X^t,$$

it is easily verified that the solution of (53), when expressed in terms of X via (52), is

$$y(X) = l_1^2\left(cV^{3/2}\sum_{r=1}^{p+1}\sum_{s=1}^{r}\sum_{t=1}^{s} a_{prst}X^t + (al_1^{-1}\,V^2 - cb_p\,V^{3/2})\log(\alpha^{-1}X+1)\right), \tag{57}$$

where the logarithm is Napierian and

$$a_{prst} = B_{prs}\,s^{-1}\binom{s}{t}\alpha^{s-t}.$$

In virtue of (49) and (54), the last equation may be written

$$a_{prst} = (-)^{s+1}\binom{p+1}{r}\binom{r}{s}\binom{s}{t}(p+1)^{-1}s^{-1}\alpha^{r-t}. \tag{58}$$

Equation (57) gives the horizontal displacement of the instrument package relative to any point in $0 \leqslant X \leqslant 1$ of the yarn supporting it, for the case of a relative

wind shear with a velocity profile given by equation (45). In particular, if δ is the horizontal displacement of the package from the balloon, as depicted in Figure 7, so that $\delta = y(1)$, equation (57) gives

$$\delta = l_1^2\left\{c\left(\sum_{r=1}^{p+1}\sum_{s=1}^{r}\sum_{t=1}^{s} a_{prst} - b_p \log(\alpha^{-1}+1)\right) V^{3/2} + a l_1^{-1} V^2 \log(\alpha^{-1}+1)\right\}. \tag{59}$$

The right-hand terms of equations (57) and (59) contain the vertical depth l_1 of the package below the balloon, the value of which is unknown at the outset since it depends upon the drag forces D_W and D_1, which vary with l_1. The value of l_1 can be determined by an iterative procedure which is described in Appendix II.

Equation (57) evidently enables the yarn deflection curve to be plotted. It also yields the locations of any points of inflection by way of the condition $\mathrm{d}^2y/\mathrm{d}X^2 = 0$.

It is clear that the effect of a relative wind shear profile of any form may be found by the method described in this section. Numerical integration of (42) and (35) may be used for any profile that does not readily admit of an analytical treatment analogous to that outlined above.

IX. A Particular Case for Wind Shear Profiles with Continuous Slopes

To illustrate the application of the foregoing results the experimental situation described in Section II is used. It involves a balloon at an altitude of 90 000 ft supporting a 2 lb wt package on a nylon yarn of stretched length

$$l = 20\,900 \text{ ft} = 6370 \text{ m}.$$

The wind shear velocity profiles given by equation (45) for the values $p = 1, 2,$ and 3 of the parameter are shown in Figure 8 for the typical case in which the height difference between the balloon and the package is

$$l_1 = 16\,400 \text{ ft} = 5000 \text{ m}. \tag{60}$$

For any other value of l_1 the different value of ρ_0 in equation (45) will alter the profiles slightly, the variations being visually undetectable for the particular maximum wind shear velocities of

$$V = 10, 20, 30, 40, \text{ and } 50 \text{ knots} \tag{61}$$

which will be considered here.

When the package is at the height 73 600 ft corresponding to equation (60), the Reynolds number of the air flow past it can be found from (37) and the values of V in (61) to lie in the range

$$3{\cdot}8\times10^4 \leqslant R \leqslant 1{\cdot}9\times10^5.$$

Since this is included in the interval (A3) of Appendix I the value of C_D in equations (38) is applicable; equation (39) then yields the air drag forces on the package and provides the values listed in the second column of Table 1.

The air drag force D_1 on the whole yarn is given by equation (47), and by taking $p = 1$, 2, and 3 in turn the total drag forces for the three velocity profiles of Figure 8 are obtained. For the particular maximum velocities given by (61) the corresponding total yarn drags summarized in the last three columns of Table 1 were obtained.

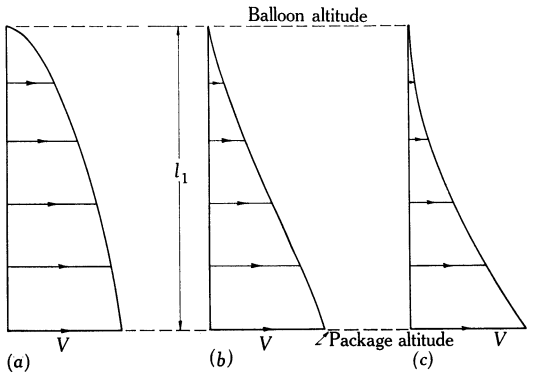

Fig. 8.—Sample velocity profiles of wind shear relative to the balloon:
(*a*) $p = 1$
(*b*) $p = 2$
(*c*) $p = 3$

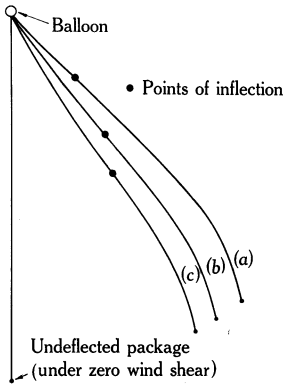

Fig. 9.—Deflected yarn and package positions corresponding to the relative wind shear velocity profiles of Figure 8 for $V = 30$ knots.

The lateral deflection δ of the package relative to the balloon is given by equation (59). For the particular experiment and profiles considered here, the iterative process described in Appendix II was used on (59) to obtain accurate values of l_1 and δ for

TABLE 1

AIR DRAG FORCES D_W ON PACKAGE AND D_1 ON WHOLE YARN

V* (knots)	D_W (kg wt)	D_1 (kg wt) for: p† = 1	2	3
10	$0{\cdot}31\times10^{-2}$	0·29	0·19	0·15
20	$1{\cdot}25\times10^{-2}$	0·82	0·55	0·41
30	$2{\cdot}80\times10^{-2}$	1·51	1·00	0·75
40	$4{\cdot}99\times10^{-2}$	2·32	1·55	1·16
50	$7{\cdot}79\times10^{-2}$	3·24	2·16	1·62

* Maximum wind shear velocity shown in Figure 8.
† $p = 1$, 2, and 3 correspond to the wind shear velocity profiles of Figures 8(*a*), 8(*b*), and 8(*c*) respectively.

each value of V given by (61). Using the initial estimate for l_1 from equation (60), one iteration gave values of δ within 10% of the true values for $V = 10$ knots and within 2% for $V = 50$ knots. A second iteration reduced these errors to less than 0·5%.

For $V = 30$ knots the final improved values of the vertical separation for the profiles of Figures 8(a), 8(b), and 8(c) were found to be respectively

$$l_1 = 4970,\ 5280,\ \text{and}\ 5510\ \text{m}.$$

TABLE 2

LATERAL DEFLECTION δ OF PACKAGE UNDER WIND SHEAR

V^* (knots)	δ (m) for: $p^* = 1$	2	3
10	1310	1030	840
20	2960	2490	2140
30	3990	3550	3200
40	4610	4260	3960
50	5010	4710	4450

* See footnotes to Table 1.

Table 2 shows the lateral deflections δ of the package relative to the balloon for each of the wind shear profiles of Figure 8 and for the maximum velocities given by (61).

Equation (57) gives the lateral deflections of points of the yarn relative to the package. For the profiles of Figure 8 it may be written as ($0 \leqslant X \leqslant 1$)

$$y(X) = a_1 X - a_2 X^2 + a_3 X^3 - a_4 X^4 - a_0 \log(\alpha^{-1} X + 1), \tag{62}$$

where the a_r are non-negative constants for each particular profile and maximum wind shear velocity. For $V = 30$ knots the values of these constants are as listed in Table 3.

TABLE 3

VALUES OF COEFFICIENTS IN EQUATION (62)

Values for $V = 30$ knots

Coefficient	p^* 1	2	3
a_0	$6{\cdot}126 \times 10^4$	$13{\cdot}116 \times 10^4$	$28{\cdot}072 \times 10^4$
a_1	$4{\cdot}174 \times 10^4$	$8{\cdot}921 \times 10^4$	$19{\cdot}076 \times 10^4$
a_2	$0{\cdot}601 \times 10^4$	$2{\cdot}081 \times 10^4$	$5{\cdot}427 \times 10^4$
a_3	0	$0{\cdot}310 \times 10^4$	$1{\cdot}408 \times 10^4$
a_4	0	0	$0{\cdot}193 \times 10^4$

* See footnote to Table 1.

Equation (62) enables the yarn deflection curves to be plotted. In view of equation (31) it also shows the inclinations of the yarn to the vertical at the package and the balloon to be respectively

$$\left(\frac{dy}{dx}\right)_{x=0} = (a_1 - a_0 \alpha^{-1}) l_1^{-1}, \tag{63}$$

$$\left(\frac{dy}{dx}\right)_{x=l_1} = \{a_1 - 2a_2 + 3a_3 - 4a_4 - a_0(1+\alpha)^{-1}\} l_1^{-1}. \tag{64}$$

In all cases the yarn is nearly vertical at its point of attachment to the package.

Figure 9 shows the yarn deflection curves (a), (b), and (c) that result from the wind shear velocity profiles of Figures 8(a), 8(b), and 8(c) respectively in the case when the maximum relative wind shear velocity is $V = 30$ knots.

The positions of the points of inflection of the yarn are shown in Figure 9. It is readily verified that such a point occurs at a height $l_1 X_1$ above the package, where X_1 is the appropriate positive root of the equation

$$(6a_4X^2 - 3a_3X + a_2)(X+\alpha)^2 - \tfrac{1}{2}a_0 = 0\,. \tag{65}$$

For $p = 1$ this is a quadratic in X; for $p = 2$ and 3 it is a cubic and quartic respectively, and was solved in these cases by successive approximations to obtain the data for Figure 9.

X. Effect of Profiles with Sharp Slope Discontinuities

Because of the occurrence in the upper atmosphere of strong horizontal winds that are confined to fairly shallow layers, it is of interest to consider the effect on the yarn and package system of wind shears possessing sharply defined boundaries. For this purpose the relative wind shear profile $v(X)$ occurring in equation (41) may be taken to be a step function of rectangular form in the interval $0 \leqslant X \leqslant 1$ corresponding to the height difference between package and balloon.

A relative wind shear profile corresponding to a single layer of air moving with uniform horizontal velocity V is given by

$$\left.\begin{aligned} v(X) &= 0\,, && 0 \leqslant X < X_1\,, \\ &= V\,, && X_1 \leqslant X \leqslant X_2\,, \\ &= 0\,, && X_2 < X \leqslant 1\,. \end{aligned}\right\} \tag{66}$$

Figures 10(a), 10(b), and 10(c) depict three particular profiles of this type.

Substitution from (66) into (41) gives the yarn drag in $(0, X)$ as

$$\left.\begin{aligned} D_X &= 0 && 0 \leqslant X < X_1\,, \\ &= \beta l_1 V^{3/2} \int_{X_1}^{X} \rho^{1/2}\,\mathrm{d}X\,, && X_1 \leqslant X \leqslant X_2\,, \\ &= \beta l_1 V^{3/2} \int_{X_1}^{X_2} \rho^{1/2}\,\mathrm{d}X\,, && X_2 < X \leqslant 1\,. \end{aligned}\right\} \tag{67}$$

From tables giving the air density ρ at various altitudes a graph of $\rho^{1/2}$ against height may be drawn. Over height variations corresponding to the shear layers of Figure 10 the graph is closely represented in $X_1 \leqslant X \leqslant X_2$ by the linear approximation

$$\rho^{1/2} = \rho_1^{1/2}\{1 - K(X - X_1)\}\,, \tag{68}$$

where ρ_1 is the density corresponding to $X = X_1$. If ρ_2 is the density for $X = X_2$,

the constant K in (68) may be found from

$$K = 1-(\rho_2/\rho_1)^{1/2}(X_2-X_1)^{-1} \tag{69}$$

for each particular choice of X_1, X_2.

For the representation (68) the integrals in (67) are easily evaluated. The resulting forms for D_X may be used in equation (35), together with $D_W = 0$ (since the package drag is plainly zero in these cases), yielding a differential equation for the yarn displacement $y(X)$ in each of the subintervals listed in (66).

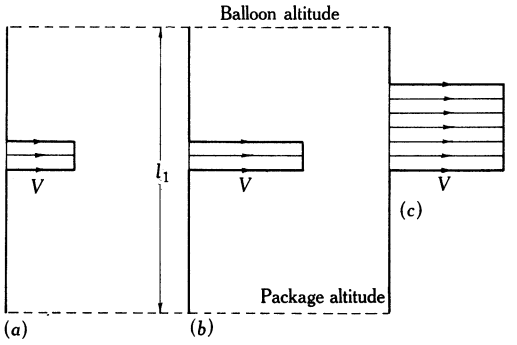

Fig. 10.—Relative wind shear velocity profiles with discontinuous slopes:
(*a*) $X_1 = 0{\cdot}5$, $X_2 = 0{\cdot}6$, $V = 30$ knots
(*b*) $X_1 = 0{\cdot}5$, $X_2 = 0{\cdot}6$, $V = 50$ knots
(*c*) $X_1 = 0{\cdot}5$, $X_2 = 0{\cdot}8$, $V = 50$ knots

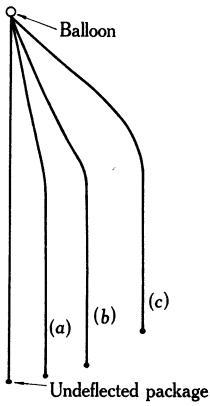

Fig. 11.—Deflected yarn and package positions corresponding to the relative wind shear velocity profiles of Figure 10.

The rest of the solution process is obvious. The differential equation for each subinterval is integrated and the integration constants are evaluated by using the initial condition $y(0) = 0$ and the continuity of $y(X)$ across the boundaries of the subintervals. It is easily verified that the solution takes the form

$$\left.\begin{aligned} y &= 0, && 0 \leqslant X < X_1, \\ &= c_1X - c_2X^2 - c_0\log(X+\alpha) + c_3, && X_1 \leqslant X \leqslant X_2, \\ &= c_0'\log(X+\alpha) - c_3', && X_2 < X \leqslant 1. \end{aligned}\right\} \tag{70}$$

Here the c_r and c_r' are positive constants expressible in terms of X_1, X_2, K, l_1, V, and the usual constants of the system, all of them being proportional to l_1^2 and $V^{3/2}$. In particular, the lateral deflection of the package is

$$\delta = c_0'\log(1+\alpha) - c_3'. \tag{71}$$

Equations (70) enable the yarn deflection curves to be plotted in the usual way. For the three relative shear velocity profiles depicted in Figure 10, which have been chosen to illustrate the effects on the yarn shape of changes in vertical scale and shear intensity, the corresponding deflection curves are as shown in Figure 11.

Comparison of Figures 10 and 11 shows that very little experience would be needed to estimate from the shape of the yarn deflection curve the nature of the wind shear structure that produces it. Greater scope for this interpretative process would be provided by further calculations of the type described in this section. For more complicated shear profiles than those of Figure 10 the integration of equation (35) could be performed numerically, but in view of the nearly linear variation of $\rho^{1/2}$ with height this would not be necessary unless the profiles selected were more complicated than the accuracy of the suggested interpretative process merits.

XI. Discussion

The experimental methods devised for determining the drag characteristics of fine woven nylon yarns (Section IV) have proved satisfactory in providing the data needed to complement the analysis of the effect of lateral wind shears on an instrument package suspended in the stratosphere. The theoretical approach has succeeded in revealing the yarn deflection curves and package displacements resulting from wind shears with various velocity profiles.

The results of the yarn drag experiments reveal some interesting features. For the range $2 \leqslant R \leqslant 100$ of Reynolds number covered, the air drag per unit length of yarn for normal flow was found to be proprtional to $v^{3/2}$ and to $d^{1/2}$, where v is the velocity of flow and d the diameter of the yarn.

The drag force on fine yarns is very much larger than casual consideration suggests. Table 2 summarizes the total drag force D_1 on a nylon yarn of diameter about 0·5 mm attached to a balloon at an altitude of 90 000 ft, and the drag force D_W on a rectangular package of sides 6, 6, and 8 in. attached to the yarn at a height of about 73 000 ft. For the three wind shear profiles depicted in Figures 8(*a*), 8(*b*), and 8(*c*) with a maximum velocity $V = 30$ knots, the ratios of yarn drag to package drag have the surprisingly large values

$$D_1/D_W = 54,\ 36,\ \text{and}\ 27$$

respectively. Viewed in another way, if the "equivalent length" l_e of yarn is defined to be that length of yarn whose drag is equal to the drag on the package (assuming the yarn drag to be uniform), then for the above three cases it is found that

$$l_e = 120,\ 180,\ \text{and}\ 240\ \text{m}$$

respectively. The displacements of the system shown in Figure 9 are therefore almost entirely the result of yarn drag, the package drag making a relatively small contribution.

The rather large lateral deflections shown in Table 2 could be of interest to physicists who conduct experiments of the suspended-package type. In the absence of any definite information to the contrary, it has hitherto been assumed that lateral deflections of the package relative to the supporting balloon are small enough to be ignored when assessing comparative data obtained by instruments at these two locations. The results of this paper suggest that it would be worth developing a balloon-based photographic method and/or a ground-based radar technique which will enable the relative positions of balloon and package to be determined accurately.

The wind shear velocity profiles depicted in Figures 8 and 10 were selected mainly because the analysis of their effects was relatively simple from a computational viewpoint. The procedure is, however, clearly applicable to velocity profiles of any form, and could be used to construct a "library" of yarn deflection outputs corresponding to various velocity profile inputs. By inversion of this transform process, the nature of the wind shear could be inferred by reference to the "library" if the form of the yarn deflection curve were known. Development of the observational technique mentioned in the preceding paragraph would therefore enable our present meagre knowledge of wind structure in the stratosphere to be greatly extended.

XII. Acknowledgments

The author is grateful to Professor V. D. Hopper of the Physics Department, RAAF Academy, for drawing his attention to the class of problems involving nylon yarns in the upper atmosphere, and to Mr. K. Maxwell of the Academy for making available the facilities of the Physics Research workshop. Thanks are also due to Flt Lt N. Mileshkin of the Academy Aeronautical Science Department for performing the nylon yarn tension test required for Section II, to F Sgt D. V. Oakley for tracing the diagrams, and to Mr. G. Baron of Fibremakers Ltd for assistance and advice in connection with the samples of nylon yarn used in the experiments described in Section IV. The management of Ampol Petroleum Pty Ltd kindly allowed the use of the unusual stairwell in their Melbourne building for the package model experiments described in Appendix I.

The author is also grateful to the referee for suggestions that greatly improved the presentation and scope of the paper.

XIII. References

Fibremakers Ltd. (1951).—Nylon in Industry. (Company publication.)

Goldstein, S. (Ed.) (1952).—"Modern Developments in Fluid Dynamics." (Oxford Univ. Press.)

Gray, D. E. (Ed.) (1963).—"American Institute of Physics Handbook." (McGraw-Hill: New York.)

Hopper, V. D., Laby, Jean E., Sparrow, J. G., and Unthank, E. L. (1963).—*Nature, Lond.* **99**, 271.

Ramsey, A. S. (1945).—"Statics." (Cambridge Univ. Press.)

Sears, W. R. (1948).—*J. aeronaut. Sci.* **15**, 49.

Appendix I

Determination of Drag Coefficient of Package

To find the drag coefficient C_D defined in equation (36), a cardboard model of geometrically similar shape to the package was dropped on its side down the stairwell of a tall building. Its terminal velocity of free fall was found by timing its descent over the latter part of its path. Equation (37) then yielded the Reynolds number R_1 for this model experiment at sea level as

$$R_1 = 1{\cdot}4 \times 10^5. \tag{A1}$$

The air drag force on the model was known, being equal (in the terminal velocity situation) to the weight of the model. Equation (36) therefore enabled the drag coefficient of the model to be calculated as

$$C_D = 1{\cdot}26\,. \tag{A2}$$

The drag coefficient of such an obstacle is almost constant (Goldstein 1952) throughout the Reynolds number range

$$2\times10^3 < R < 2{\cdot}5\times10^5\,, \tag{A3}$$

within which the measured value in (A1) lies. From hydrodynamic similarity theory (Goldstein 1952), the value of C_D in (A2) will apply also to the instrument package in the stratospheric situation provided the Reynolds numbers of the air flow lie within the range (A3). It is easily verified that this condition is satisfied for all the wind shears considered in this paper, thus justifying the use in equations (38) and (39) of the value of C_D quoted in equation (A2) above.

Appendix II

Determination of Depth of Package below Balloon

The vertical separation l_1 between the instrument package and balloon may be determined by the following iterative process.

Equation (59) may be written as

$$\delta/l_1^2 = K(\theta)\,, \tag{A4}$$

where $K(\theta)$ denotes the factor in braces on the right-hand side of (59) and (as shown in Fig. 7) θ is the angular deflection of the package from the vertical. The dependence of K on θ is by way of the quantity l_1 occurring in it, since from Figure 7 it can be seen that

$$l_1 = \mathrm{OB}\cos\theta \simeq l\cos\theta\,, \tag{A5}$$

the last approximation being reasonable if the curvature of the yarn is not excessive.

It can be seen from Figure 7 that

$$\delta = l_1\tan\theta\,, \tag{A6}$$

and, on dividing (A6) by (A5), that

$$\delta/l_1^2 = (\tan\theta)/(l\cos\theta)\,. \tag{A7}$$

On equating the right-hand sides of (A4) and (A7) one readily finds that

$$\sin^2\theta + 2\gamma\sin\theta - 1 = 0\,, \tag{A8}$$

where

$$\gamma = \{2K(\theta)\,l\}^{-1}\,. \tag{A9}$$

The relevant solution of (A8) is

$$\sin\theta = (\gamma^2+1)^{1/2} - \gamma\,. \tag{A10}$$

A process of successive approximations may now be used to obtain θ (and hence l_1 from (A5) and δ from (A6)) to any desired accuracy. One begins by using in (A5) any initial estimate for θ (even $\theta = 0$ will serve); then first estimates can be obtained for l_1 from (A5), δ from (A6), $K(\theta)$ from (A4), γ from (A9), and for the right-hand side of (A10). Solving (A10) for θ then yields a second approximation for θ, whence second estimates of all other quantities by repetition of the foregoing sequence.

When the value of l_1 has been refined sufficiently by this method it may be used in (A6) to yield the package deflection δ and in equation (57) to give the yarn deflection curve.

If judgement is used in making the first estimate of θ, a single iteration of the above type is enough to yield results of sufficient accuracy for practical purposes. The great rapidity of convergence of the process results from the deliberate extraction of the factor l_1^2 in the right-hand side of equation (59); the iterated quantity l_1 is thereby restricted to appear inside the braces of (59) in a term that is much smaller in magnitude than those to which it is added.

Appendix III

Estimation of Maximum Error in Calculated Deflections

The maximum error involved in the prediction of the yarn and package deflections under wind shear is estimated by compounding the maximum errors in the quantities leading to or appearing in the deflection formulae (62) and (70). As the determination of many of these quantities was not by way of repeated observations an accurate assessment of the probable error cannot be made, but it will certainly be much less than the maximum value established below.

The equation (7) for the yarn slope may be written as

$$\mathrm{d}y/\mathrm{d}x = (W+ws)^{-1}(D_W+D_X)\,, \tag{A11}$$

where the package and yarn drag forces are given by

$$D_W = \tfrac{1}{2}C_D\rho_0 SV^2 \tag{A12}$$

and

$$D_X = \int_0^s F\,\mathrm{d}s = \int_0^x D\,\mathrm{d}x = \tfrac{1}{2}kd^{1-n}\mu^n l_1 \int_0^X \rho^{1-n}v^{2-n}\,\mathrm{d}X\,. \tag{A13}$$

In (A13), the error in l_1 will be that in l, which is given by equation (2) as

$$l = l_0\{1+\lambda^{-1}(W+\tfrac{1}{2}w_0 l_0)\}\,. \tag{A14}$$

Assumptions involved in the analysis include:

(i) that C_D is constant in (A12); the estimated error in this assumption, together with that in the experimental C_D value, is 15%.

(ii) that in (A13) the Sears independence principle $F = D\cos\psi$ is valid; the estimated error (based on the validity test of Section IV) is 5%.

Approximations and numerical values used include:

(iii) $s = lX$ to facilitate integration of (A11); by measurements made from Figures 9 and 11 the error is 6·7%.

(iv) w is constant along yarn; from the Section II result that $w_{\min} = 0{\cdot}947\, w_0$ the maximum error (from the mean) is 2·7%.

(v) $d^{1/2}$ is constant along yarn; from the Section II result that $d_{\min} = 0{\cdot}973\, d_0$ the maximum error of $d^{1/2}$ (from the mean) is 1·2%.

(vi) $\mu^{1/2}$ is constant over the height spanned by the yarn; from tables of μ values, the maximum error (from the mean) is 1%.

(vii) $n = 0{\cdot}5$; the error is 3%.

(viii) $k = 10{\cdot}1$; the error is 3%.

(ix) $\lambda = 27{\cdot}0$ kg wt; the error is 6%.

All other values used are effectively exact (e.g. W, $w_0 l_0$, S), or irrelevant to an error analysis (e.g. ρ_0, l_0, V).

From (A12) and (i)

$$\text{error in } D_W = 15\%. \tag{A15}$$

From (A14) and (ix), allowing for relative magnitudes,

$$\text{error in } l_1 = 0{\cdot}3\%. \tag{A16}$$

From (vii), the errors in ρ^{1-n} and V^{2-n} (for $V = 50$ knots) in (A13) are 4·1% and 5% respectively, so that

$$\text{error in integrand of (A13)} = 9{\cdot}1\%. \tag{A17}$$

From (A13), (ii), (v), (vi), (viii), (A16), and (A17),

$$\text{error in } D_X = 5+1{\cdot}2+1+3+0{\cdot}3+9{\cdot}1 = 19{\cdot}6\%. \tag{A18}$$

From (iii) and (iv), allowing for relative magnitudes,

$$\text{error in } (W+ws)^{-1} = 3{\cdot}8\%. \tag{A19}$$

From (A11), (A15), (A18), and (A19), allowing for relative magnitudes,

$$\text{error in } \mathrm{d}y/\mathrm{d}x = 3{\cdot}8+0{\cdot}0244\times 15+19{\cdot}6 = 23{\cdot}8\%. \tag{A20}$$

From (A11), (A16), and (A20),

$$\text{error in deflection } y = 0{\cdot}3+23{\cdot}8 = 24{\cdot}1\%. \tag{A21}$$

This final value of 24% is the total maximum error. The total probable error is difficult to estimate as the error assessments of most quantities were not based on repeated observations, but the subjective judgement of 15% appears reasonable.